IEEE Access
Multidisciplinary ⋮ Rapid Review ⋮ Open Access Journal

Received August 17, 2020, accepted August 28, 2020, date of publication September 10, 2020, date of current version September 29, 2020.

Digital Object Identifier 10.1109/ACCESS.2020.3023345

Energy Comparison of Controllers Used for a Differential Drive Wheeled Mobile Robot

ALEXANDR STEFEK[1], THUAN VAN PHAM[1], VACLAV KRIVANEK[2], (Member, IEEE), AND KHAC LAM PHAM[3]

[1]Department of Air Defence, University of Defence, 66210 Brno, Czech Republic
[2]Department of Military Robotics, University of Defence, 66210 Brno, Czech Republic
[3]Department of Aircraft Technology, University of Defence, 66210 Brno, Czech Republic

Corresponding author: Thuan Van Pham (vanthuan.pham@unob.cz)

This work supported by the Czech Republic Ministry of Defence (University of Defence in Brno development program ''Research of sensor and control systems to achieve battlefield information superiority'').

ABSTRACT In order to select the best controller for a Differential Drive Wheeled Mobile Robot (DDWMR), an energy consumption comparison relating to tracking accuracy is used as a very strict criterion. Therefore, this paper reviews some well-known controllers designed for the DDWMR. Furthermore, there are presented several experiments with the extensible open-source code programmed in Python. Such an extensible open-source code presentation could serve as a tool for simulating, comparing, and evaluating a set of different control algorithms. The kinematic and dynamic models of the DDWMR and control algorithms are implemented in this open-source code to determine a travel time, a distance between the robot's position and a given path, a linear velocity, an angular velocity, a travel path length, and a total kinetic energy loss of the DDWMR. These simulation results are used to compare and evaluate the given control algorithms. Moreover, the simulation results also enable to answer the question of whether a significant increase in energy consumption is worth shortening the travel path by just a bit. Finally, this paper includes a direct link to the stored experiments which are runnable and could serve as a proof. Besides, users can also easily supplement with other controllers and different paths to evaluate robot tracking control algorithms.

INDEX TERMS Differential drive robots, energy model, fitness function, kinetic energy, robot's energy, wheeled mobile robot control.

I. INTRODUCTION

Robotic Science has been developing rapidly due to its various useful applications in many aspects of common life, industry, medicine, the military, and especially its ability to operate in hazardous and toxic environments. Recently, the Differential Drive Wheeled Mobile Robot (DDWMR) has been increasingly noticed and widely applied within the scope of Robotic Science. It has a lot of advantages, such as flexible motion capabilities, a simple structure, lower production costs. Furthermore, it can operate independently for a long time without a direct human control.

The DDWMR has some different forms, such as a 2-wheel, a 3-wheel, or a 4-wheel type. We can find the 2-wheel type in [13], the 3-wheel type in [5], [7], [10], [11], [18]–[20], [23], and the 4-wheel type in [15], [17]. The 3-wheel type is the most popular form which comprises of two fixed powered wheels mounted on both left and right side of the robot platform and one passive castor wheel used for balance and stability.

The motion control algorithm of the DDWMR: In principle, the movement of the DDWMR is based on two separately driven wheels placed on either side of the robot body. Therefore, it changes its direction by changing the relative rotation speed of the two wheels. For the DDWMR, the problems of path planning and path tracking are the most important. However, the path tracking is more important because its accuracy directly affects the robot operability. Many authors have researched and published various control algorithms of path tracking for the DDWMR, such as the adaptive output feedback control [2], the input-output feedback linearization method [4], the two-step feedback linearization control [3], the backstepping-based control [5], the PID control [6], the Lyapunov function-based control [8], [9], the adaptive and sliding mode control [7], [10], [11], [18], the neural-network-based control [19], and the robust adaptive-based control [21]. All of the above studies refer only to continuous or smooth curves, whereas the energy consumption of the robot is not mentioned. In reality, robots often have to work in

The associate editor coordinating the review of this manuscript and approving it for publication was Yingxiang Liu.

complex conditions (environments with many obstacles, slipping wheels, acceleration of robots varies when they move) over a long time. So in many cases, it is too difficult for the robot to track the given path smoothly with saved energy consumption.

A requirement for the DDWMR is that it has to move smoothly, with no or minimum vibration, and detects a minor tracking error while tracking the sharp turn path or the discontinuous path. In order to achieve that requirement, the robot needs to have a constant rotation of the two wheels or it has to move on a path in a circular arc format. However, it should be mentioned that the circular arc function does not fit all possible paths, which the robot might be required to take [12]. These problems have been studied and solved by several different control algorithms that were presented in some papers, such as the controllers proposed by Kanayama and Robins Mathew [1], a feedback-based control for circular path [12], the Lyapunov-based method [25], a clever trigonometry-based control [24], a fuzzy logic control [24], and a Dubins path-based control [16].

The comparison and evaluation of the given control algorithms can be based on many different criteria, such as the distance between the robot's position and the given path (the cross-track error), the travel distance (the length of the path), the total energy loss, the travel time, etc. For the mobile robot motion control, accuracy and energy consumption are always strict criteria. So it is necessary to have a simulator to verify and compare these criteria when the different controllers are used. Therefore, this paper aims at simulating, and comparing the results of some well-known control algorithms for the 3-wheel DDWMR to track the sharp turn path or the discontinuous path in the same working conditions. Then the best controller will be designed to improve it so that the robot suits each working condition and specific working environment.

This paper is organized as follows: some different shapes, a kinematic model, a dynamic model, and an energy model of the DDWMR are introduced in Section II; a review of some well-known control algorithms used for the DDWMR is provided in Section III; simulation, result collection, comparison, and the used control algorithms evaluation in Section IV. A summary and a conclusion complete the paper in Section V.

II. DIFFERENTIAL DRIVE WHEELED MOBILE ROBOTS

Wheeled mobile robots are employed for inventory management, factory automation, military surveillance, etc. These robots are classified into different categories, such as car-like robots, omnidirectional robots, and differential drive robots; of which differential drive robots are a prominent class [1].

A. POPULAR SHAPES OF THE DIFFERENTIAL DRIVE WHEELED MOBILE ROBOT

Currently, the structure of the DDWMR has many different types, such as a 2-wheel, a 3-wheel, or a 4-wheel differential drive mobile robot, as shown in Fig. 1. Each one has different advantages but the 3-wheel type has more advantages than the others.

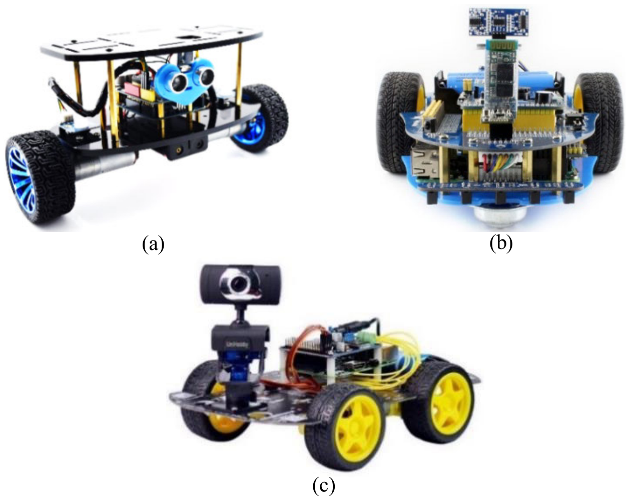
(a)

(b)

(c)

FIGURE 1. (a) a 2-wheel differential drive mobile robot, (b) a 3-wheel differential drive mobile robot, (c) a 4-wheel differential drive mobile robot.

In this study, we mention only the 3-wheel DDWMR type because it is widely used in many applications, such as industrial automated guided vehicles and service robots. Furthermore, the robots of this type are controlled more easily than others and provide high maneuverability and rotation around the center of the robot [11]. Besides, the 3-wheel DDWMR has a simple structure and is suitable for many practical applications as well as being popular and prevailing in the market.

B. MODELS OF A 3-WHEEL DIFFERENTIAL DRIVE MOBILE ROBOT TYPE

1) KINEMATIC MODEL

The Differential Drive Wheeled Mobile Robots (DDWMRs) usually have two independently driven wheels and one or more unpowered wheels at the rear as a balance. An important issue of the differential driving of mobile robots which needs considering is that their motion controller design is mostly based on kinematic models. The main reason is that dynamic models are more complex than kinematic models and mobile robots usually use only the low speed of the motor to control the loop [1].

The geometry and kinematic parameters of this robot are shown in Fig. 2.

In Fig. 2, this robot is the DDWMR which has important parameters as below:

v is the linear velocity of the DDWMR (ms^{-1}),
θ is the orientation of the DDWMR (rad),
ω_r is the angular velocity of the right wheel (rads^{-1}),
ω_l is the angular velocity of the left wheel (rads^{-1}),
v_r is the linear velocity of the right wheel (ms^{-1}),
v_l is the linear velocity of the left wheel (ms^{-1}),
r is the radius of the right and the left wheels (m),
b is the distance between the right and the left wheels (m),

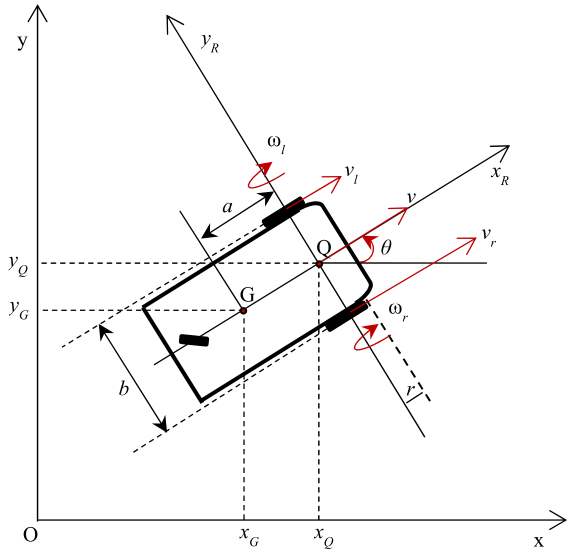

FIGURE 2. A geometry of a 3-wheel differential drive mobile robot.

Q is the center of the axis between the right and the left wheels,
G is the center of gravity of the DDWMR,
a is the distance between Q and G (m).

The kinematic model equations depend on the geometrical structure of the DDWMR [3]. However, most of the 3-wheel DDWMRs have the same kinematic equation which is constructed as follows [3], [5], [12], [13], [15]:

$$x_G = x_Q - a\cos\theta \tag{1}$$

$$y_G = y_Q - a\sin\theta \tag{2}$$

We assume that [3], [13]:

- The wheels are rolling without slipping,
- The center of gravity G coincides with the point Q,
- The guidance axis is perpendicular to the robot plane.

Based on Fig. 2 we get:

$$v_r = v + \frac{b}{2}\dot{\theta} \tag{3}$$

$$v_l = v - \frac{b}{2}\dot{\theta} \tag{4}$$

Adding and subtracting (3) and (4) we get:

$$v = \frac{1}{2}\left(v_r + v_l\right) \tag{5}$$

$$\dot{\theta} = \frac{1}{b}\left(v_r - v_l\right) \tag{6}$$

Due to the non-slipping assumptions we have $v_r = r\omega_r$ and $v_l = r\omega_l$.

From Fig. 2 we get:

$$\dot{x} = \dot{x}_Q = v\cos\theta \tag{7}$$

$$\dot{y} = \dot{y}_Q = v\sin\theta \tag{8}$$

$$\dot{\theta} = \omega \tag{9}$$

Equations (7), (8) and (9) are a kinematic model of the 3-wheel DDWMR.

2) MOTOR DYNAMICS

A dynamic model of motor behavior has to be modelled to consider its characteristic on the robot chassis [12].

The DC motors are usually used for the DDWMR. The motor dynamics is modelled as follows [30]:

The electrical circuit and the free body diagram of the motor rotor of a DC motor are depicted in Fig.3.

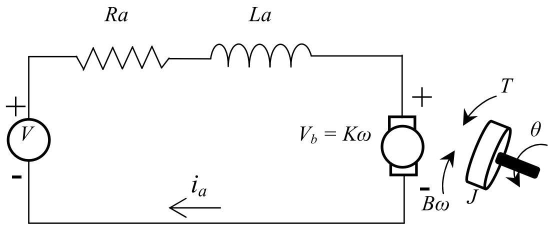

FIGURE 3. A basic electrical circuit of a DC motor and a free body diagram of the motor rotor.

An equation governing the mechanical dynamics of the motor is

$$J\ddot{\theta} + B\dot{\theta} = K_t i_a \tag{10}$$

The armature current has its own dynamics. From Fig. 3, we can write

$$L_a\frac{di_a}{dt} + R_a i_a = V - K_e\dot{\theta} \tag{11}$$

where J is the moment of inertia, θ is the angle of rotation of the output shaft, $T = K_t i_a$ is the mechanical torque developed in the motor rotor, K_t is the armature constant, i_a is the armature current, B is the damping coefficient, V is the input voltage, K_e is the motor constant, R_a stands for the armature resistance, and L_a is the armature inductance.

The Laplace transform of (10) and (11) are given as:

$$Js^2\theta(s) + Bs\theta(s) = K_t I_a(s) \tag{12}$$

$$L_a s I_a(s) + R_a I_a(s) = V(s) - K_e s\theta(s) \tag{13}$$

From (12) and (13) we get

$$Js^2\theta(s) + Bs\theta(s) = K_t\frac{V(s) - K_e s\theta(s)}{R_a + sL_a} \tag{14}$$

The transfer function of the angular velocity $\omega(s)$ to the input voltage $V(s)$ is

$$F(s) = \frac{\omega(s)}{V(s)} = \frac{K_t}{(R_a + L_a s)(Js + B) + K_t K_e} \tag{15}$$

Two identical motors are used for one robot chassis, so only one transfer function of the motor will be defined.

$$F(s) = \frac{\omega(s)}{V(s)} = \frac{\frac{K_t}{L_a J}}{s^2 + \frac{R_a J + L_a}{L_a J}s + \frac{R_a B + K_t K_e}{L_a J}} \tag{16}$$

Or:

$$F(s) = \frac{b_1}{s^2 + a_0 s + a_1}$$

where $b_1 = \frac{K_t}{L_a J}$; $a_0 = \frac{R_a J + L_a}{L_a J}$; $a_1 = \frac{R_a B + K_t K_e}{L_a J}$

C. FITNESS FUNCTION

There are many kinds of fitness functions for a mobile robot, but this paper only presents behavioral fitness functions for the 3-wheel Differential Drive Wheeled Mobile Robots. In this case, we consider the behavior of the robots in relation to their energy consumption and their travel distance because the amount of energy consumption and the travel distance affects the uptime and ability to perform their tasks.

1) ENERGY MODEL OF DIFFERENTIAL DRIVE WHEELED MOBILE ROBOT

Overall Energy Model of the Differential Drive Wheeled Mobile Robot: After analyzing all lost components, the complete energy model equation is presented as [22]:

$$E_{battery} = E_{dc} + E_k + E_{friction} + E_{elect} \tag{17}$$

where E_{dc} is the energy loss for DC motor, E_k is the kinetic energy losses, $E_{friction}$ is the energy losses due to friction, E_{elect} is the energy losses in the electronics, $E_{battery}$ is the energy of battery used for the robot.

In this study, we only consider the kinetic energy losses of the robot and ignore the other components.

The kinetic energy of the robot at any time can be expressed as [29]:

$$E_k = \frac{1}{2}m\left(v(t)\right)^2 + \frac{1}{2}I\left(\omega(t)\right)^2 \tag{18}$$

From (18), the total kinetic energy loss from the initial time to the final time is

$$\begin{aligned}\sum E_k &= \sum_{t_0}^{t_n}\left(\frac{1}{2}m\left(v(t)\right)^2 + \frac{1}{2}I\left(\omega(t)\right)^2\right)\\ &= \sum_{i=0}^{z}\left(\frac{1}{2}m\left(v(t_0+i\Delta T)\right)^2 + \frac{1}{2}I\left(\omega(t_0+i\Delta T)\right)^2\right)\end{aligned} \tag{19}$$

where t, t_0, t_n represent time, initial time, and final time respectively, m and I denote the mass and the moment of inertia of the robot, $i = (0, 1, 2, 3, \ldots., z = (t_n - t_0)/\Delta T), \Delta T$ is step time.

2) TRAVEL DISTANCE

The robot travel distance is an important quantity used for evaluating the quality of moving along the track of the given path. The less the difference between the travel distance and the length of the given path is, the less the average of cross-track error is. In this study, we expect the average cross-track error to be as small as possible. So, the travel distance is as similar to the length of the given path as possible. The function of the travel distance is

$$S = \int_{t_0}^{t_n} |v(t)|dt \tag{20}$$

where S is the travel distance by the robot, t_0 and t_n represent the initial time and final time, respectively.

In this paper, (19) and (20) are used as the fitness functions to calculate energy consumption and travel distance that are used to compare and evaluate the controllers based on the energy consumption in relation to the travel distance of the robot.

III. WELL-KNOWN MOTION CONTROL ALGORITHMS

Motion is an important activity of the Differential Drive Wheeled Mobile Robot. Controlling the DDWMR movement depends on the structure of the robot, on the task that it will perform, and on the environment in which it will move. Therefore, choosing suitable algorithms for robot motion control depends on each specific case.

Currently, there are a lot of different motion control methods for the DDWMR, such as problems of position (posture) tracking, trajectory (path) tracking, point to point tracking and leader following. Among them, the path tracking is of more concern. In the trajectory tracking problems, a reference point (the midpoint between the left and right wheel) on the robot must follow a desired trajectory in the Cartesian space starting from a given initial configuration. Some prevalent algorithms of the DDWMR path tracking are the adaptive output feedback control algorithm, the input-output feedback linearization method, the backstepping control method, the PID control, the Lyapunov-based control, the sliding mode-based control, the robust control method, the adaptive fuzzy control, the neural-network control, and the vision-based methods, etc.

Point to point motion control or waypoint tracking of a robot: the robot must move to a desired goal configuration from a given initial configuration. As mentioned in the introduction of this paper, the DDWMR needs to move smoothly and minimize error tracking even when it tracks the sharp turn path or the discontinuous path. Some well-known point to point motion controllers have been proposed, such as the feedback-based controller for circular path, the Dubins path-based controller, the Lyapunov-based controller, the clever trigonometry-based controller, the advance controller by Robins Mathew, and by the Kanayama's controller, etc.

A. FEEDBACK-BASED CONTROLLER FOR CIRCULAR PATH

According to [12] and kinematic model (7), (8), (9) we get:

$$\begin{aligned}\dot{x} &= \dot{x}_Q = v\cos\theta\\ \dot{y} &= \dot{y}_Q = v\sin\theta\\ \dot{\theta} &= \omega = \frac{v_r - v_l}{b} = \frac{2\Delta}{b}\end{aligned}$$

where $v = \frac{v_r+v_l}{2}$; $\Delta = \frac{v_r-v_l}{2}$, b is the distance between the right and the left wheel.

The DDWMR moves from point A to point B. Based on feedback control, the [12] shows that:

$$\dot{\theta} = \omega = \frac{2\Delta}{b} = 2v\frac{(AB)_x\sin\theta - (AB)_y\cos\theta}{|AB|^2} \tag{21}$$

In the (21)

$$\overrightarrow{AB} = \left((AB)_x\,;\,(AB)_y\right),\ |AB| = \sqrt{\left((AB)_x^2 + (AB)_y^2\right)}$$

$(AB)_x$ is the projection of AB along the x-axis. $(AB)_y$ is the projection of AB along the y-axis.

The kinematic model with the angular velocity of the robot in (21) is a form of feedback-based controller for the DDWMR moving on a circular path segment.

The paper [12] introduces one advanced control law by adding a coefficient K_c to (21), so we get:

$$\dot{\theta} = \omega = \frac{2\Delta}{b} = K_c 2v \frac{(AB)_x \sin\theta - (AB)_y \cos\theta}{|AB|^2} \tag{22}$$

Coefficient K_c is greater than zero. (22) allows the running of multiple experiments and fine-tuning a path of a robot on a single line segment [12].

B. THE LYAPUNOV-BASED CONTROLLER

The DDWMR moves from point Q with linear velocity v and orientation θ to point G, depicted in Fig. 4.

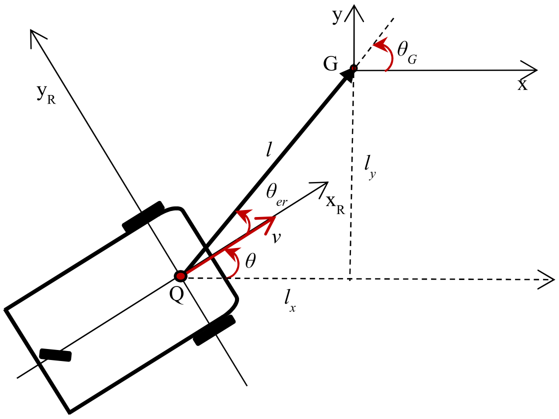

FIGURE 4. A geometry of a 3-wheel differential drive wheeled mobile robot moves to a goal.

Based on the Lyapunov function, the linear velocity and the angular velocity of the DDWMR are calculated as following [13], [25]:

$$v = v_{ri} \cos\theta_{er} \tag{23}$$

$$\omega = k_1\theta_{er} + \frac{v_{ri}\cos\theta_{er}\sin\theta_{er}\,(\theta_{er} + k_2\theta_G)}{\theta_{er}} \tag{24}$$

where v_{ri} is a linear reference velocity of the robot, coefficient k_1, k_2 are greater than zero, θ_{er}, θ, θ_G = atan2(l_y, l_x) are the steering angle, the angle, and the robot orientation, respectively.

C. CLEVER TRIGONOMETRY-BASED CONTROLLER

In this case, we need to move the DDWMR from the starting point to the destination point, as in Fig. 5.

A new point $\tilde{X} = (\tilde{x}, \tilde{y})$ is positioned a small distance l directly in front of X. The point $\tilde{X}$ can simultaneously move forward, perpendicular and rotate. X is close to $\tilde{X}$ and once we align the robot with our target destination $\theta = \theta_G$ (here θ is the orientation of the robot, θ_G is the orientation of the goal) then X will pass over the location of $\tilde{X}$ shortly after $\tilde{X}$ gets to next location [23].

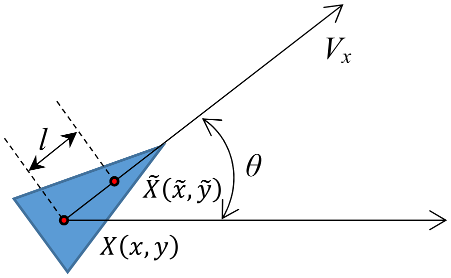

FIGURE 5. A geometry of a 3-wheel differential drive wheeled mobile robot moves to a goal base on trigonometry.

From Fig. 5, we get:

$$\tilde{x} = x + l\cos\theta \Rightarrow \dot{\tilde{x}} = \dot{x} - l\sin\theta \tag{25}$$

$$\tilde{y} = y + l\sin\theta \Rightarrow \dot{\tilde{y}} = \dot{y} + l\cos\theta \tag{26}$$

By substituting $\dot{x}, \dot{y}$ in (25), (26) for $\dot{x}, \dot{y}$ in (7), (8) and presented in [23] we get:

$$v = v_{ri}\cos(\theta_G - \theta) \tag{27}$$

$$\omega = \frac{v_{ri}}{l}\sin(\theta_G - \theta) \tag{28}$$

where v_{ri} is the desired forward velocity, an expected input for steering the robot towards a goal, l is the distance from X to $\tilde{X}$. It is considered as a coefficient of the controller.

The l needs to tune. In general, a shorter value of l makes the robot turn quicker, but a longer l allows the robot to run more smoothly [23].

D. ADVANCED CONTROLLER BY KANAYAMA AND ROBINS MATHEW

In Fig. 6, the DDWMR follows a path connecting the waypoints from a source $q_{w0} = (x_{w0}, y_{w0})$ to a destination $q_{wn} = (x_{wn}, y_{wn})$ through a set of intermediate waypoints $q_{wk} = (x_{wk}, y_{wk})$, $k = 1, 2, \ldots,$ n $- 1$ [1]. In the paper [1], Robins Mathew has mentioned the controller proposed by Kanayama, which is one of the most popular controllers in case of trajectories with continuous curvature. This control equation is given in (29) and (30). Further, Robins Mathew proposes a new control method to make the DDWMR tightly track the line connecting the waypoints with a minor cross-track error.

The control law of Kanayama is given below:

$$v_{ci} = v_{ri}\cos\theta_{ie} + k_1 x_{ie} \tag{29}$$

$$\omega_{ci} = \omega_{ri} + k_2 v_{ri} y_{ie} + k_3 v_{ri}\sin\theta_{ie} \tag{30}$$

The control law of Robins Mathew is given below:

$$v_{ci} = v_{ri}\cos\theta_{ie} \tag{31}$$

$$\omega_{ci} = \omega_{ri} + k_1 v_{ri} T_{ie} + k_2 v_{ri}\sin\theta_{ie} \tag{32}$$

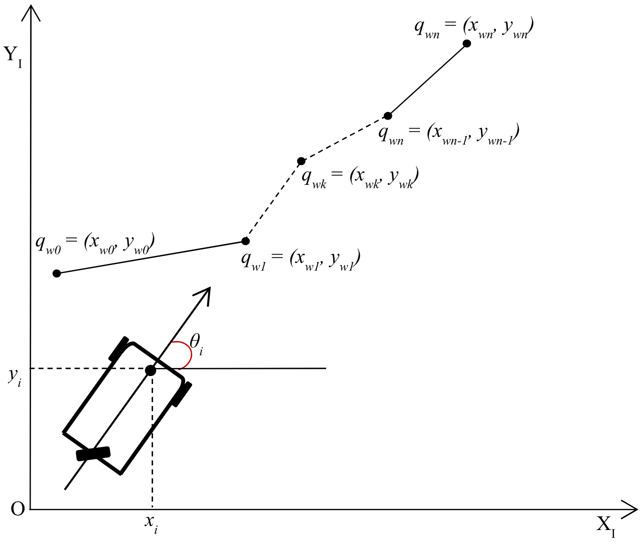
$q_{wn} = (x_{wn}, y_{wn})$
Y_I
$q_{wn} = (x_{wn-1}, y_{wn-1})$
$q_{wk} = (x_{wk}, y_{wk})$
$q_{w0} = (x_{w0}, y_{w0})$
$q_{w1} = (x_{w1}, y_{w1})$
θ_i
y_i
O
x_i
X_I

FIGURE 6. The robot tracking waypoints trajectory.

In (29) – (32), v_{ci}, ω_{ci}, v_{ri}, ω_{ri}, are the linear, the angular velocity, the linear reference, the angular reference velocity respectively, $(k_1, k_2, k_3) > 0$ are the control gains, (x_i, y_i, θ_i) is the current robot position, and $(x_{wk}, y_{wk}, \theta_{wk})$ is waypoint posture, $(x_{ie}, y_{ie}, \theta_{ie})$ is the robot posture error, where $x_{ie} = (x_{wk} - x_i), y_{ie} = (y_{wk} - y_i), \theta_{ie} = (\theta_{wk} - \theta_i)$, $T_{ie} = (x_i - x_{wk})\sin\phi - (y_i - y_{wk})\cos\phi$ is the cross-track error, ϕ is defined as the angle made by the line connecting current waypoint with the previous waypoint.

E. DUBINS PATH – BASED CONTROLLER

Dubins curve consists of several circular segments and straight segments. The shortest Dubins curve consists of three circular segments and straight segments. The primary forms are: (RSL, LSL, RSR, LSR, RLR, LRL). Where L, R represent the circular turning to the left and right respectively, S represent the tangent connecting two turning circulars [16].

The primary forms (RSL, LSL, RSR, LSR, RLR, LRL) of the Dubins path form are presented in Fig. 7.

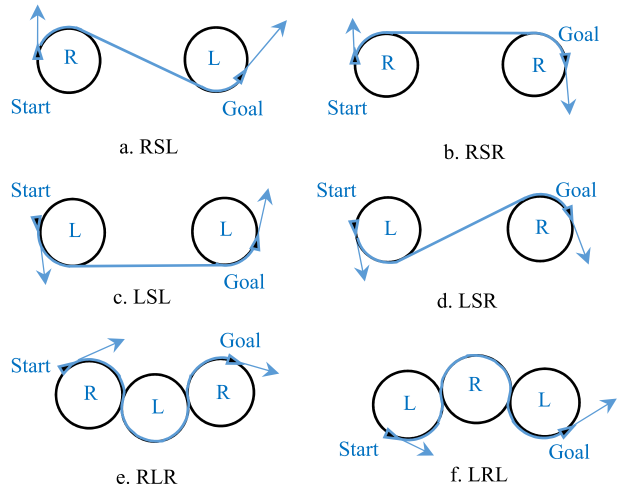

a. RSL

b. RSR

c. LSL

d. LSR

e. RLR

f. LRL

FIGURE 7. The Dubins path tracking.

TABLE 1. Input parameters of the robot.

Parameters	Value
Wheel's radius (*r*)	0.0925 m
Distance between 2 driven wheels (*b*)	0.37 m
Mass of the robot (m)	9 kg
Moment of inertia of the robot (*I*)	0.16245 kgm^2
Start position of the robot on x axis (start_x)	0 m
Start position of the robot on y axis (start_y)	0 m
Start orientation of the robot (start_θ)	45°
Moment of inertia of the rotor (*J*)	0.01 kgm^2/s^2
Damping ratio (*B*)	0.1 Nms
Electromotive force constant (*K* = *Kt* = *Ke*)	0.01 Nm/A
Electrical Resistance (*Ra*)	0.1 Ω
Electrical Inductance (*La*)	0.01 H

TABLE 2. Coefficients of controllers.

Coefficients	Value
Feedback-based controller for circular path with G = 4	
Coefficient: k_1	4.0
Feedback-based controller for circular path with G = 8	
Coefficient: k_1	8.0
The Lyapunov-based controller	
Coefficient: k_1	5.0
Coefficient: k_2	0.01
Clever Trigonometry-based controller	
Coefficient: k_1	7.0
Advanced controller by Robins Mathew	
Coefficient: k_1	1.5
Coefficient: k_2	6.5
Advanced controller by Kanayama	
Coefficient: k_1	0.001
Coefficient: k_2	0.1
Coefficient: k_3	5.0
Dubins path–based controller	
Minimal rotation radius: k_1	1.0

IV. RESULTS AND DISCUSSION

A. SIMULATING AND RESULTS COLLECTING

The input parameters of the robot used for simulation in this study are shown in Table 1.

The coefficients of the controllers are given in Table 2. Two different given paths are used to simulate the behavior of the robot. The first one is a square path with parameters given in Table 3 and the second one is a straightforward path that has a different angle at any waypoints of the path. The parameters of the straightforward path are given in Table 4.

The movement of a mobile robot will be directly affected by the speed that its actuator can provide. If the provided velocity is too large, it will cause some difficulty in tracking, a high tracking error, and a high energy loss. Conversely, if the provided velocity is too small, the robot will move too slowly so it may affect its performance. Therefore, in this study, the velocity will be limited to evaluate and compare the quality of the used controllers. Then the value of the provided velocity will be changed to investigate and evaluate the effect

TABLE 3. Parameters of a square path.

Waypoints	x-axis (m)	y-axis (m)
0	0	0
1	10	0
2	10	10
3	0	10
4	0	0

TABLE 4. Parameters of a straightforward path.

Waypoints	x-axis (m)	y-axis (m)
0	0	0
1	10	0
2	20	10
3	30	10
4	25	20

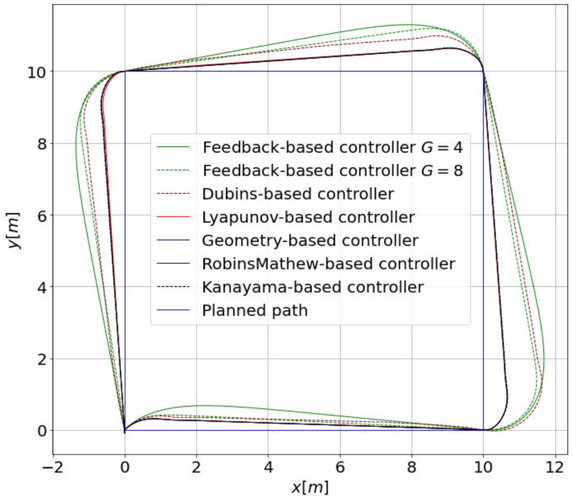

FIGURE 8. The square path tracking of the robot.

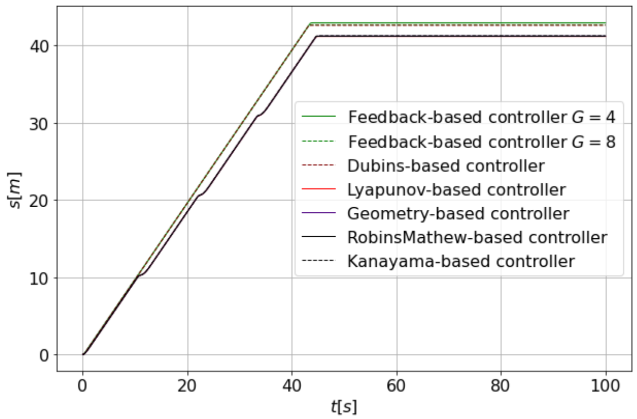

FIGURE 9. Travel distance over time of the robot when tracking the square path.

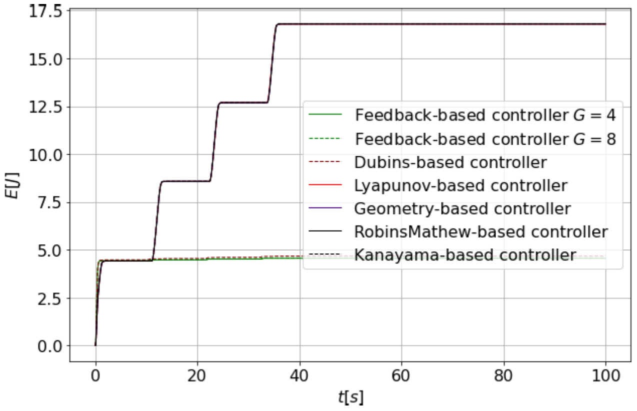

FIGURE 10. Kinetic energy loss over time of the robot when tracking the square path.

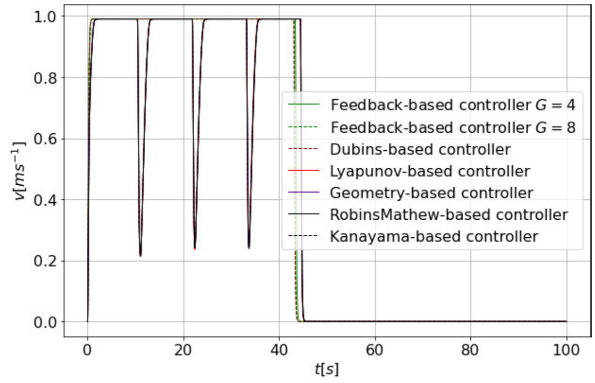

FIGURE 11. Linear velocity over time of the robot when tracking the square path.

of the velocity change on the motion quality and energy loss of the robot.

This simulation creates some experiments of these are three main experiments presented below:

The first experiment proves that using the input parameters given in Tables 1-4, the linear reference velocity $v_{ri} = 1.0$ ms^{-1}, the angular reference velocity $\omega_{ri} = 0$ rads^{-1}, the linear and the angular velocity of the controllers are limited (v is limited in the range [0.2 ms^{-1} to 1.0 ms^{-1}], ω is also limited in the range [-0.75 rads^{-1} to 0.75 rads^{-1}]). Running the simulation, we will receive some important results shown in Figures 8 to 17 and in Tables 5 and 6 below:

The second experiment testifies that using the Lyapunov-based controller with the input parameters given in Tables 1–4, the linear reference velocity $v_{ri} = 1.0$ ms^{-1}, 1.1 ms^{-1}, 1.15 ms^{-1}, the angular reference velocity $\omega_{ri} = 0$ rads^{-1}, the linear and angular velocity of the controllers are limited too. When $v_{ri} = 1.0$ ms^{-1}, v is limited in the range [0.2 ms^{-1} to 1.0 ms^{-1}]. When $v_{ri} = 1.1$ ms^{-1}, v is limited in the range [0.2 ms^{-1} to 1.1 ms^{-1}], and when $v_{ri} = 1.15$ ms^{-1}, v is limited in the range [0.2 ms^{-1} to 1.15 ms^{-1}]. ω is limited in the range [-0.75 rads^{-1} to 0.75 rads^{-1}]). Running the simulation, we will receive some important results, shown in Figures 18 and 19 and Tables 7 and 8 below:

Some important results of the third experiment are shown in Figure 20 and Table 9 below:

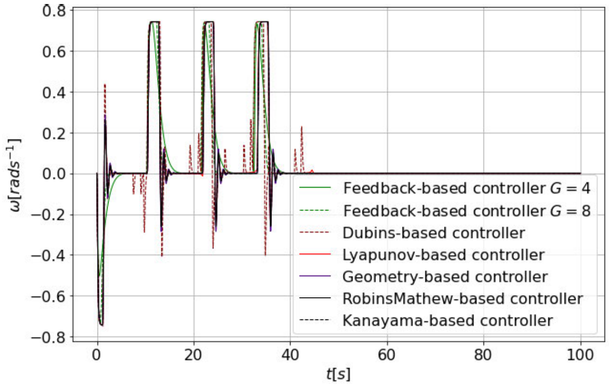

FIGURE 12. Angular velocity over time of the robot when tracking the square path.

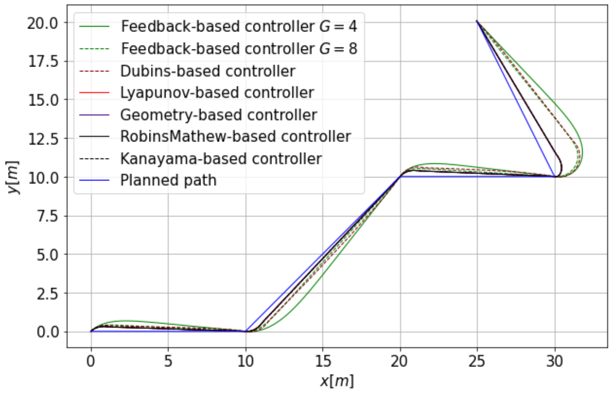

FIGURE 13. The straightforward path tracking of the robot.

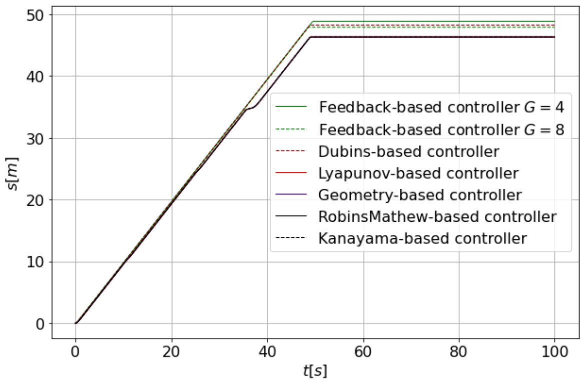

FIGURE 14. Travel distance over time of the robot when tracking the straightforward path.

The third experiment above proves that using input parameters given in Tables 1, 3, 4, and adding some more waypoints in each segment of the straightforward path. The linear reference velocity $v_{\text{ri}} = 1.0 \text{ ms}^{-1}$, the angular reference velocity $\omega_{\text{ri}} = 0 \text{ rads}^{-1}$, linear and angular velocity of the controllers are limited (v is limited in range [0.2 ms^{-1} to 1.0 ms^{-1}], ω is limited in range [-0.75 rads^{-1} to 0.75 rads^{-1}].

We can also see the results in some extra experiments as follows:

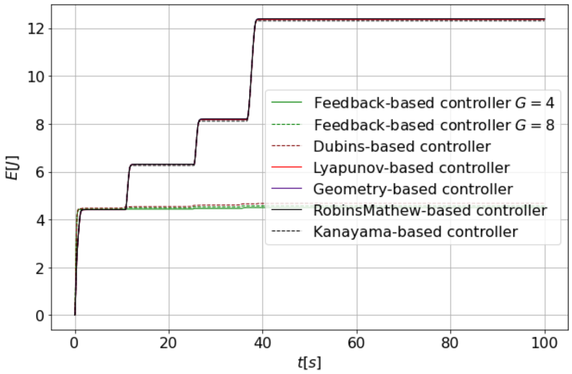

FIGURE 15. Kinetic energy loss over time of the robot when tracking the straightforward path.

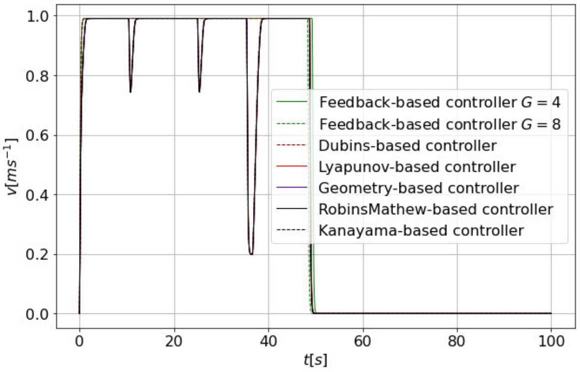

FIGURE 16. Linear velocity over time of the robot when tracking the straightforward path.

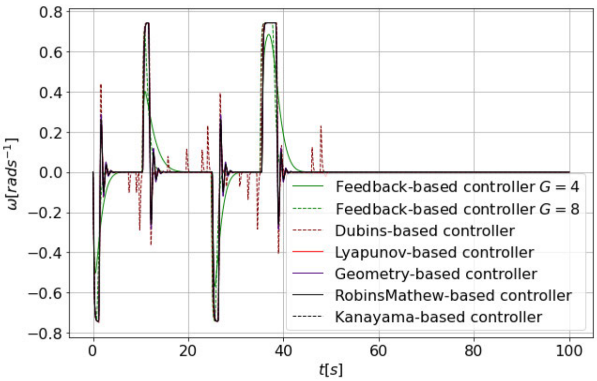

FIGURE 17. Angular velocity over time of the robot when tracking the straightforward path.

The extra experiment 1: A diamond-shape path tracking of the robot. The results of the experiment are shown in Figure 21 and Table 10.

The extra experiment 2: A sharp turn path tracking of the robot. The results of the experiment are shown in Figure 22 and Table 11.

In order to compare the energy loss of other controllers, we add some more different controllers and paths to the

TABLE 5. The travel distance and energy consumption of the robot when tracking the square path.

Control method	Travel Distance (m)	Travel Distance in percentage (%)	Energy (J)	Energy in percentage (%)
Feedback-based G = 4	42.9522	104.2871	4.5525	100.0000
Feedback-based G = 8	42.6893	103.6488	4.5723	100.4349
Dubins-based	42.6272	103.4980	4.6736	102.2660
Lyapunov-based	41.1865	100.0000	16.7825	368.6436
Geometry-based	41.2230	100.0886	16.7934	368.8830
Robins Mathew-based	41.2231	100.0889	16.7935	368.8852
Kanayama-based	41.2694	100.2013	16.8015	369.0610

TABLE 6. The travel distance and energy consumption of the robot when tracking the straightforward path.

Control method	Travel Distance (m)	Travel Distance in percentage (%)	Energy (J)	Energy in percentage (%)
Feedback-based G = 4	48.8373	105.5207	4.4990	100.0000
Feedback-based G = 8	47.8826	103.4579	4.5672	101.5159
Dubins-based	48.2384	104.2267	4.6736	103.8809
Lyapunov-based	46.3365	100.1173	12.3635	274.8055
Geometry-based	46.2822	100.0000	12.3904	275.4034
Robins Mathew-based	46.2823	100.0002	12.3902	275.3990
Kanayama-based	46.3050	100.0493	12.3081	273.5741

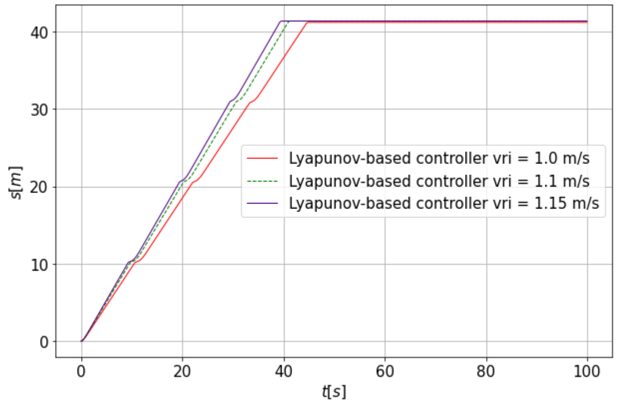

FIGURE 18. Travel distance over time of the robot controlled by Lyapunov-based control to track the square path.

open-source code programmed in Python. The program will show us all of the results.

B. DISCUSSION

1) THE USED CONTROL METHODS COMPARING AND EVALUATING

From these simulation results, it can be seen that when the robot tracks the square path or the straightforward path, its travel distance and energy loss are different when the different control algorithms are used in each segment of the given path. Therefore, the total travel distance and total energy loss are different when the robot is controlled by the different control algorithms to move in a full path, as shown in Tables 5-8 and in Fig.8-10, Fig.13-15 above.

In more detail, Table 5 indicates that when the robot is controlled to track the square path based on the ‘‘Lyapunov-based controller’’, and the straightforward path based on the ‘‘geometry-based control’’ algorithm, its travel distance is the smallest of all.

When it is controlled based on the ‘‘feedback-based controller for the circular path G = 4’’, the travel distance is the smallest in comparison with the travel distance based on the other control algorithms. When it is controlled by the rest of the control algorithms, the travel distance is variable and depends on each kind of the given path.

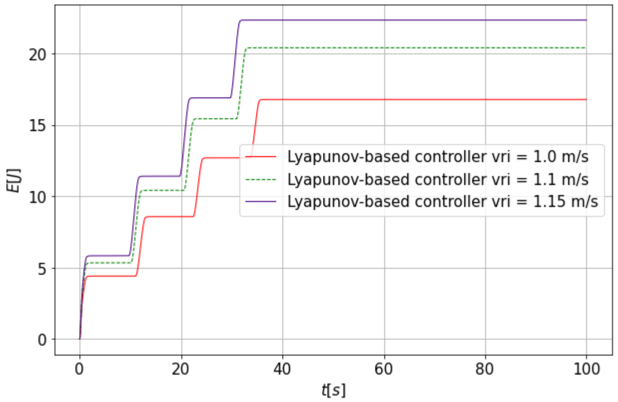

FIGURE 19. Kinetic energy loss over time of the robot controlled by Lyapunov-based control to track the square path.

TABLE 7. The travel distance and energy consumption of the robot when tracking the square path by “Lyapunov-based controller”.

Control method	Travel Distance (m)	Travel Distance in percentage (%)	Energy (J)	Energy in percentage (%)
Lyapunov-based controller v_{ri} = 1.0 ms^{-1}	41.1865	100.0000	16.7825	100.0000
Lyapunov-based controller v_{ri} = 1.1 ms^{-1}	41.3576	100.4154	20.4061	121.5915
Lyapunov-based controller v_{ri} = 1.15 ms^{-1}	41.3469	100.3895	22.3438	133.1375

TABLE 8. The travel distance and energy consumption of the robot when tracking the straightforward path by “Lyapunov-based controller”.

Control method	Travel Distance (m)	Travel Distance in percentage (%)	Energy (J)	Energy in percentage (%)
Lyapunov-based controller v_{ri} = 1.0 ms^{-1}	46.3365	100.0000	12.3635	100.0000
Lyapunov-based controller v_{ri} = 1.1 ms^{-1}	46.4588	100.2639	15.0661	121.8595
Lyapunov-based controller v_{ri} = 1.15 ms^{-1}	46.5251	100.4070	16.5161	133.5876

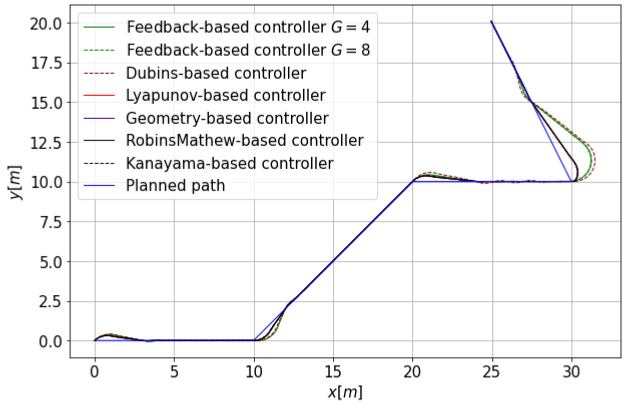

FIGURE 20. The many waypoints tracking of the robot.

TABLE 9. The travel distance and energy consumption of the robot when tracking the straightforward path with many Waypoints.

Control method	Travel Distance (m)	Travel Distance in percentage (%)	Energy (J)	Energy in percentage (%)
Feedback-based G = 4	47.8720	103.3970	5.4863	100.0000
Feedback-based G = 8	47.7120	103.0515	6.5392	119.1914
Dubins-based	48.5032	104.7603	5.7471	104.7537
Lyapunov-based	46.2992	100.0000	12.3509	225.1226
Geometry-based	46.3300	100.0665	12.3929	225.8881
Robins Mathew-based	46.3392	100.0864	12.3264	224.6760
Kanayama-based	46.3058	100.0143	12.3388	224.9020

TABLE 10. The travel distance and energy consumption of the robot when tracking the diamond-shape path.

Control method	Travel Distance (m)	Travel Distance in percentage (%)	Energy (J)	Energy in percentage (%)
Feedback-based G = 4	48.3481	105.3900	4.5127	100.0000
Feedback-based G = 8	47.7540	100.0950	4.5870	101.6465
Dubins-based	48.2184	105.1073	4.6845	103.8070
Lyapunov-based	45.9903	100.2505	13.2607	293.8529
Geometry-based	45.9428	100.1470	13.2009	292.5278
Robins Mathew-based	45.9429	100.1471	13.2009	292.5278
Kanayama-based	45.8754	100.0000	13.1446	291.2802

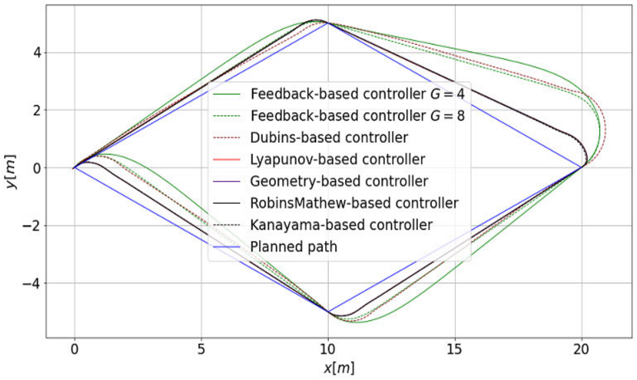

FIGURE 21. A diamond-shape path tracking of the robot.

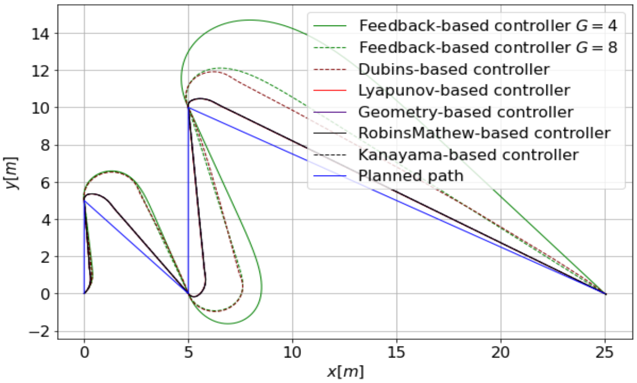

FIGURE 22. A sharp turn path tracking of the robot.

TABLE 11. The travel distance and energy consumption of the robot when tracking the sharp turn path.

Control method	Travel Distance (m)	Travel Distance in percentage (%)	Energy (J)	Energy in percentage (%)
Feedback-based G = 4	54.6847	123.9257	4.5380	100.0000
Feedback-based G = 8	50.5263	114.5020	4.5910	101.1679
Dubins-based	50.7001	114.8959	4.6777	103.0785
Lyapunov-based	44.1270	100.0000	16.9625	373.7880
Geometry-based	44.1457	100.0424	16.9640	373.8211
Robins Mathew-based	44.1464	100.0440	16.9640	373.8211
Kanayama-based	44.1658	100.0879	16.9782	374.1340

Besides, from Table 5, Table 6, and Fig. 8, Fig. 13 it is obvious that the trajectory of the robot is always the furthest from all the segments of the given path when control is based on the ‘‘feedback-based controller for the circular path G = 4’’. In other words, the average of the error-track is the biggest when the robot is controlled based on the ‘‘feedback-based controller for the circular path G = 4’’. The cross-track average of the robot is the smallest when control is based on the ‘‘Lyapunov-based controller’’ to track the square path, and the cross-track average of the robot is the smallest when it is controlled based on the ‘‘geometry-based controller’’ to track the straightforward path. Thus, it is very intuitive to recognize and compare the travel distances by the robot when it is controlled by the respective controllers shown in Table 5, Table 6, and Fig.8, Fig.13. It is also evident that the cross-track error in each segment is dependent on not only the control algorithms used but also the angle created by two contiguous segments. The smaller that angle is, the bigger the cross-track error is.

Therefore, if we evaluate the robot control quality based on the criterion of the travel distance, the control algorithm of the ‘‘Lyapunov-based controller’’ is the best when the robot tracks the square path, and the ‘‘geometry-based controller’’ is the best when the robot tracks the straightforward path because the travel distance is the smallest. The control algorithm "feedback-based controller for the circular path G = 4" is the least qualified, because the travel distance is the largest.

The [23] mentioned mobile robots rely on a battery as their power source for most of the time. However, batteries have a very limited energy capacity. This finite amount of energy leads to a very short operational time of the robot, which may not be enough for missions or tasks that require more time and energy to be completed. Therefore, despite the intelligence and capabilities, their use in such tasks is not feasible. Although the time of operation can be prolonged by increasing the number of batteries or by diverting the robot back to the charging station, both of these techniques come at the expense of the increased cost and size which can cause control problems. Another way to increase the time of operation in robots is by reducing the energy consumption in the robot system itself and thus increasing their energy efficiency [23]. So, using less energy is considered as a very important criterion to evaluate the quality of control algorithms for the robot. It means that the less energy the robot uses, the better control algorithm is.

According to the energy loss criterion and based on Table 5, 6, Fig.10, Fig. 15 it can be seen that the "feedback-based controller for circular path G = 4" algorithm is the best because the total energy loss is the smallest of all. The "Kanayama-based controller" is the worst when the robot tracks the square path, and the "geometry-based controller" is the worst when the robot tracks a straightforward path because the total energy loss is the most significant of all.

In this research, the Lyapunov, Robins Mathew, geometry, and Kanayama-based controllers are called the high energy controllers. The feedback-based controller for a circular path and the Dubins path-based controller are called the low energy controllers. It is also evident that when the robot is controlled by the high energy controllers, the energy consumption is significantly more excessive (more than 270%) than the energy consumption of the robot controlled by the low energy controllers. Meanwhile, when the robot is controlled by the high energy controllers the length of the travel path is only slightly shorter than when it is controlled by low energy controllers (less than 5.5207%). So it can be said that when the robot is controlled to track a given path, the high energy consumption has to increase (greater than 270%) to shorten only a little (less than 5.5207%), which is unnecessary in most robot missions. When it is necessary to reduce the length of the travel path, we need to improve the control algorithms to shorten the length of the travel path with no increase of energy loss or negligible increase of energy loss.

2) USING ONLY ONE CONTROLLER WITH DIFFERENT REFERENCE LINEAR VELOCITY

When the robot is controlled by only the "Lyapunov-based controller", it is set on different values of the reference linear velocity. Based on Table 7, Table 8, and Fig.18, Fig.19 it can be found that the faster linear velocity increases, the bigger the energy loss is in both types of the given paths. It means the robot will move and reach the destination faster, but its total energy loss becomes greater.

In this case, it is clear that when the linear velocity is set from 1.0 ms-1 to 1.1 ms-1 and then goes up to 1.15 ms-1, the travel time is reduced significantly (about 5s) and the energy loss greatly increases (more than 20%) while the increase in the travel distance is negligible (less than 0.4154%). Thus, to shorten the travel time, the robot must increase energy consumption significantly. This result has raised a question if the use of high velocity is so important in case that higher energy must be provided. So, based on the specific tasks of the robot, users can decide to increase energy consumption significantly, or not, so that the robot can quickly move to its destination.

3) MORE WAYPOINTS ADDED INTO THE SEGMENTS OF THE GIVEN PATHS

When some more waypoints are added into the segments of the given paths, the robot will track that path tightly. So the cross-track error of the robot will be reduced significantly.

Figure 20 and Table 9 show that the travel distance will be increased, or reduced, while the cross-track error will be reduced and most of the total energy loss will increase a lot. This result also has raised a question, if the decrease of the cross-track error is so important that higher energy must be provided. The answer to that question depends on the specific tasks of the robot. If the robot has to track the given path tightly, it must increase energy consumption significantly. In this way, the robot can reduce its cross-track error. But in some tasks where the robot does not have to track the given path tightly, it is unnecessary to increase the energy consumption to reduce its cross-track error.

C. OPEN-SOURCE CODE TO IMPLEMENT EXPERIMENTS

This paper proposes an open-source code as a tool from https://colab.research.google.com/drive/1UP2ru4v51peFy9jO650vh8tFQTtlJCMd which was programmed with Python language in Jupyter Notebook to implement and compare the different control algorithms introduced in section 3. Users must click on this link to open the simulation program. However, to edit it, users have to copy it to their google drive by clicking the "Copy to Drive" or "File > Save a copy in Drive". After that, they must get access to https://drive.google.com/drive/u/0/my-drive to open and edit that copy of the simulation program by using Google Colaboratory.

This program consists of an inevitable program initialization section, a robot model, simulation tools, controllers, a simulation section, an interactive simulation and a simulation results section.

1) THE INEVITABLE PROGRAM INITIALIZATION SECTION

This section declares some libraries (NumPy, Math, SciPy. Integrate, matplotlib. pyplot, etc.) used for programming in the next sections.

2) THE ROBOT MODEL SECTION

The Robot model section introduces some different shapes of the DDWMR, robot parameters, basic equations used for the DDWMR, the kinematic model, kinematic model implementation, the dynamic model, and dynamic model implementation. Users can change the robot parameters in this section for their own robot parameters.

3) THE SIMULATION TOOLS SECTION

Simulation tools are used for numerical computation RK45 function from SciPy library. They consist of computation, given path, robot model and controller connection, closure function for simulation, simulation runner, path plotter, value plotter, all in one plotter, and data extractor.

4) THE CONTROLLERS SECTION

The controllers section allows users to add some controllers or define their own control algorithm at ''Define your controller here''. That function will return the velocity and omega value of the robot.

5) THE SIMULATION SECTION

The simulation section allows users to definite square path, straightforward path, or put their own path. In this section, the experiment is described and executed.

In the ''Experiment Description'', users can change the value of velocity limitation and also can change the value of the coefficients in the controllers.

6) THE INTERACTIVE SIMULATION SECTION

In the Interactive Simulation section, you can choose different experiment sets on different paths by selecting different ''experimTag'' and ''pathTag''.

7) THE SIMULATION RESULTS SECTION

In this section, users can get the simulation text results, change the simulation image output size, simulate all graphs in one figure, simulate the path time, simulate the travel distance over time, and simulate the robot kinetic energy loss over time.

Thus, it is clear that this open-source code allows users to use different types of paths for the robot by defining them in the section ''Simulation'' and subsection ''Paths Definition''. At the same time, it also allows users to use other control algorithms by adding or modifying the codes in the section ''Controllers'' and subsection ''Define your controller here''.

V. SUMMARY AND CONCLUSION

In this paper, the set of various well-known controllers for the differential driven robot has been discussed. As a main attribute of those controllers, the model of energy consumption has been taken into account. Visually, the ability to track the given path is important and thus the differences of the energy consumptions have been evaluated in relation to differences in the total lengths of travel paths. According to the carried experiments, the controllers from a group of the low energy controllers have been offering significantly less energy consumption and still considerable precision in the tracking of the given path. The experiments have shown that the shortage of the travel path is less than 5 percent while energy consumption is almost more than 200 percent. The comparison of low energy controllers and high energy controllers has raised a question if the advantages of high energy controllers are so crucial their real usage. As the comparison always matters, standard and open tools should be used. Such tools allow us to build a rich database of experiments and transparent comparison of any given controller with the old and already proven one. To support this idea the software has been developed with the use of the Google Colab® and Jupyter platforms and opened for all users.

In our future research, we will focus on improving a motion control algorithm for the DDWMR that tracks a given path with higher accuracy, less energy loss but smooth movement without or less vibration and a shorter travel time. The result will be tested by using this open-source code program.

REFERENCES

[1] R. Mathew and S. S. Hiremath, ''Development of waypoint tracking controller for differential drive mobile robot,'' in *Proc. 6th Int. Conf. Control, Decis. Inf. Technol. (CoDIT)*, Paris, France, Apr. 2019, pp. 1121–1126.

[2] X. Zhou, B. Ma, and L. Yan, ''Adaptive output feedback tracking controller for wheeled mobile robots with unmeasurable orientation,'' in *Proc. 37th Chin. Control Conf. (CCC)*, Wuhan, China, Jul. 2018, pp. 412–417.

[3] M. Yallala and S. J. Mija, ''Path tracking of differential drive mobile robot using two step feedback linearization based on backstepping,'' in *Proc. Int. Conf. Innov. Control, Commun. Inf. Syst. (ICICCI)*, Greater Noida, India, Aug. 2017, pp. 1–6.

[4] N. V. Tinh, N. T. Linh, P. T. Cat, P. M. Tuan, M. N. Anh, and N. P. T. Anh, ''Modeling and feedback linearization control of a nonholonomic wheeled mobile robot with longitudinal, lateral slips,'' in *Proc. IEEE Int. Conf. Autom. Sci. Eng. (CASE)*, Fort Worth, TX, USA, Aug. 2016, pp. 996–1001.

[5] D. Diaz and R. Kelly, ''On modeling and position tracking control of the generalized differential driven wheeled mobile robot,'' in *Proc. IEEE Int. Conf. Automatica (ICA-ACCA)*, Curico, Chile, Oct. 2016, pp. 1–6.

[6] J. Meng, A. Liu, Y. Yang, Z. Wu, and Q. Xu, ''Two-wheeled robot platform based on PID control,'' in *Proc. 5th Int. Conf. Inf. Sci. Control Eng. (ICISCE)*, Zhengzhou, China, Jul. 2018, pp. 1011–1014.

[7] S. Peng and W. Shi, ''Adaptive fuzzy output feedback control of a nonholonomic wheeled mobile robot,'' *IEEE Access*, vol. 6, pp. 43414–43424, 2018.

[8] Y. Jinhua, Y. Suzhen, and J. Xiao, ''Trajectory tracking control of WMR based on sliding mode disturbance observer with unknown skidding and slipping,'' in *Proc. 2nd Int. Conf. Cybern., Robot. Control (CRC)*, Chengdu, China, Jul. 2017, pp. 18–22.

[9] F.-G. Rojas-Contreras, A.-I. Castillo-Lopez, L. Fridman, and V.-J. Gonzalez-Villela, ''Trajectory tracking using continuous sliding mode algorithms for differential drive robots,'' in *Proc. IEEE 56th Annu. Conf. Decis. Control (CDC)*, Melbourne, VIC, Australia, Dec. 2017, pp. 6027–6032.

[10] B. B. Mevo, M. R. Saad, and R. Fareh, ''Adaptive sliding mode control of wheeled mobile robot with nonlinear model and uncertainties,'' in *Proc. IEEE Can. Conf. Electr. Comput. Eng. (CCECE)*, Quebec City, QC, Canada, May 2018, pp. 1–5.

[11] P. Petrov and V. Georgieva, ''Adaptive velocity control for a differential drive mobile robot,'' in *Proc. 20th Int. Symp. Electr. App. Technol. (SIELA)*, Bourgas, Bulgaria, Jun. 2018, pp. 1–4.

[12] A. Štefek, V. Křivánek, Y. T. Bergeon, and J. Motsch, ''Differential drive robot: Spline-based design of circular path,'' *Dynamical Systems: Theoretical and Experimental Analysis* (Springer Proceedings in Mathematics & Statistics), vol. 182, J. Awrejcewicz, Ed. Cham, Switzerland: Springer, 2016, pp. 331–342.

[13] S. G. Tzafestas, *Introduction to Mobile Robot Control*, 1st ed. Amsterdam, The Netherlands: Elsevier, 2014, sec. 5, pp. 159–169.

[14] A. L. Nelson, G. J. Barlow, and L. Doitsidis, ''Fitness functions in evolutionary robotics: A survey and analysis,'' *Robot. Auto. Syst.*, vol. 57, no. 4, pp. 345–370, Apr. 2009, doi: 10.1016/j.robot.2008.09.009.

[15] R. L. S. Sousa, M. D. do Nascimento Forte, F. G. Nogueira, and B. C. Torrico, ''Trajectory tracking control of a nonholonomic mobile robot with differential drive,'' in *Proc. IEEE Biennial Congr. Argentina (ARGENCON)*, Buenos Aires, Argentina, Jun. 2016, pp. 1–6.

[16] B. Shi, Y. Su, C. Wang, L. Wan, and Y. Qi, ''Recovery path planning algorithm based on dubins curve for autonomous underwater vehicle,'' in *Proc. IEEE 8th Int. Conf. Underwater Syst. Technol., Theory Appl. (USYS)*, Wuhan, China, Dec. 2018, pp. 1–5.

[17] M. Begnini, D. W. Bertol, and N. A. Martins, ''A robust adaptive fuzzy variable structure tracking control for the wheeled mobile robot: Simulation and experimental results,'' *Control Eng. Pract.*, vol. 64, pp. 27–43, Jul. 2017, doi: 10.1016/j.conengprac.2017.04.006.

[18] S. Peng and W. Shi, ''Adaptive fuzzy output feedback control of a nonholonomic wheeled mobile robot,'' *IEEE J. Control Eng. Pract.*, vol. 64, pp. 27–43, 2018, doi: 10.1109/ACCESS.2018.2862163.

[19] M. Yue, L. Wang, and T. Ma, ''Neural network based terminal sliding mode control for WMRs affected by an augmented ground friction with slippage effect,'' *IEEE/CAA J. Automatica Sinica*, vol. 4, no. 3, pp. 498–506, Jul. 2017.

[20] H. Yang, X. Fan, P. Shi, and C. Hua, ''Nonlinear control for tracking and obstacle avoidance of a wheeled mobile robot with nonholonomic constraint,'' *IEEE Trans. Control Syst. Technol.*, vol. 24, no. 2, pp. 741–746, Mar. 2016, doi: 10.1109/TCST.2015.2457877.

[21] L. Xin, Q. Wang, J. She, and Y. Li, ''Robust adaptive tracking control of wheeled mobile robot,'' *Robot. Auto. Syst.*, vol. 78, pp. 36–48, Apr. 2016, doi: 10.1016/j.robot.2016.01.002.

[22] M. Wahab, F. Rios-Gutierrez, and A. El Shahat, ''Energy modeling of differential drive robots,'' in *Proc. SoutheastCon*, Fort Lauderdale, FL, USA, Apr. 2015, pp. 1–6.

[23] S. Armah, S. Yi, and T. A. Lebdeh, ''Implementation of autonomous navigation algorithms on two-wheeled ground mobile robot,'' *Amer. J. Eng. Appl. Sci.*, vol. 78, pp. 36–48, Apr. 2016, doi: 10.3844/ajeassp.2014.149.164.

[24] L. A. Yekinni and A. Dan-Isa, ''Fuzzy logic control of goal-seeking 2-Wheel differential mobile robot using unicycle approach,'' in *Proc. IEEE Int. Conf. Autom. Control Intell. Syst. (I2CACIS)*, Selangor, Malaysia, Jun. 2019, pp. 300–304.

[25] P. Xinzhe, L. Zhiyuan, P. Run, and C. Hong, ''Practical stabilization of wheeled mobile robots based on control Lyapunov function,'' in *Proc. Int. Conf. Control Appl.*, Glasgow, U.K., Sep. 2002, pp. 345–349.

[26] H. Chitsaz, S. M. LaValle, D. J. Balkcom, and M. T. Mason, ''Minimum wheel-rotation paths for differential-drive mobile robots,'' in *Proc. IEEE Int. Conf. Robot. Autom. (ICRA)*, Orlando, FL, USA, May 2006, pp. 1616–1623.

[27] X. Song and S. Hu, ''2D path planning with dubins-path-based A* algorithm for a fixed-wing UAV,'' in *Proc. 3rd IEEE Int. Conf. Control Sci. Syst. Eng. (ICCSSE)*, Beijing, China, Aug. 2017, pp. 69–73.

[28] M. Elbanhawi, M. Simic, and R. N. Jazar, ''Continuous path smoothing for car-like robots using B-Spline curves,'' *J. Intell. Robotic Syst.*, vol. 80, no. S1, pp. 23–56, Jan. 2015, doi: 10.1007/s10846-014-0172-0.

[29] S. Liu and D. Sun, ''Minimizing energy consumption of wheeled mobile robots via optimal motion planning,'' *IEEE/ASME Trans. Mechatronics*, vol. 19, no. 2, pp. 401–411, Apr. 2014, doi: 10.1109/TMECH.2013.2241777.

[30] P. B. Deb, O. Saha, S. Saha, and S. Paul, ''Dynamic model analysis of a DC motor in MATLAB,'' *IJSER J. Int. J. Sci. Eng. Res.*, vol. 8, no. 2, pp. 57–60, Mar. 2017.

ALEXANDR STEFEK received the M.Sc. degree *(summa cum laude)* in command automation, and electronic computers, and the Ph.D. degree from the Military Academy, Czech Republic, in 1994 and 1998, respectively. His research interest includes stochastic optimization.

THUAN VAN PHAM received the engineer's degree and the master's degree in cybernetics and automation engineering from Le Quy Don University, Hanoi, Vietnam, in 2007 and 2015, respectively. He is currently pursuing the Ph.D. degree in technical cybernetics and mechatronics with the University of Defence, Brno, Czech Republic. His research interests include intelligent sensing and control, embedded computers, navigation for mobile robot, motion control of wheeled mobile robots, and intelligent control systems.

VACLAV KRIVANEK (Member, IEEE) received the M.Sc. degree in control and guidance systems of missiles from the Military Academy Brno, Czech Republic, in 2002, the Mastèrè Spécialisé degree in techniques for aeronautics and space from SUPAERO, Toulouse, France, in 2006, and the Ph.D. degree in diagnostic methods from the University of Defence (UoD), Brno, Czech Republic, in 2010. From 2011 to 2019, he was a Member with the Department of Air Defence, UoD. Since 2020, he has been a Lecturer with the Department of Military Robotics, UoD. His research interests include feed-back control systems applied to the air defence systems and mobile robot design.

KHAC LAM PHAM received the engineer's degree in informatics and control systems from Bauman Moscow State Technical University, Moscow, Russia, in 2010. He is currently pursuing the Ph.D. degree in electrical engineering with the University of Defence, Brno, Czech Republic. His research interests include design and control of electric drivers for UAV using battery.